AGU PUBLICATIONS

JGR

Journal of Geophysical Research: Earth Surface

RESEARCH ARTICLE
10.1002/2015JF003491

Key Points:
- Simulation reproduces downstream sediment budget and bed texture
- Bed fining allowed rapid evacuation of tailings with little proximal aggradation
- Uncertainty in model details and initial state allowed for by control run

Correspondence to:
R. I. Ferguson,
r.i.ferguson@durham.ac.uk

Citation:
Ferguson, R. I., M. Church, C. D. Rennie, and J. G. Venditti (2015), Reconstructing a sediment pulse: Modeling the effect of placer mining on Fraser River, Canada, *J. Geophys. Res. Earth Surf.*, *120*, doi:10.1002/2015JF003491.

Received 16 FEB 2015
Accepted 5 JUL 2015
Accepted article online 14 JUL 2015

Reconstructing a sediment pulse: Modeling the effect of placer mining on Fraser River, Canada

R. I. Ferguson[1], M. Church[2], C. D. Rennie[3], and J. G. Venditti[4]

[1]Department of Geography, Durham University, Durham, UK, [2]Department of Geography, University of British Columbia, Vancouver, British Columbia, Canada, [3]Department of Civil Engineering, University of Ottawa, Ottawa, Ontario, Canada, [4]Department of Geography, Simon Fraser University, Burnaby, British Columbia, Canada

Abstract Gold mining along 525 km of the Fraser River between 1858 and 1909 added an estimated 1.1×10^8 t of tailings, half gravel and the rest finer, to the river's natural sediment load. We simulate the response using a 1-D multigrain size morphodynamic model. Since premining conditions are unknown and modern data are insufficient for tuning the process representation, we devised a novel modeling strategy which may be useful in other data-poor applications. We start the model from a smoothed version of the modern longitudinal profile with bed grain size distributions optimized to match alternative assumptions about natural sediment supply and compare runs that include mining with control runs that can be used to quantify the effects of deficiencies in process representation and initialization. Simulations with an appropriate choice of natural supply rate closely match the best available test data, which consist of a detailed 1952–1999 gravel budget for the distal part of the model domain. The simulations suggest that the main response to mining was rapid bed fining, which allowed a major increase in bed load transport rate with only slight (~0.1 m) mean aggradation within the mining region and most of the excess sediment exported well beyond the mountain front within the mining period or soon afterward. We compare this pattern of response by a large, powerful river with previous case studies of river adjustment to sediment supply change.

1. Introduction

Any major increase in the supply of bed load to a river is offset, and perhaps eventually matched, by an increase in transport capacity. This is achieved by changes in one or more of channel slope, morphology, and bed texture. In many documented examples the initial response was significant aggradation, followed by some combination of translation and dispersion of the topographic high in what has variously been termed a sediment "wave" [*Gilbert*, 1917; *Lisle et al*., 1997; *Lisle*, 2008], "slug" [*Nicholas et al*., 1995], or "pulse" [*Cui and Parker*, 2005]. This style of response has been observed following mining [e.g., *Gilbert*, 1917; *James*, 1989; *Knighton*, 1989], landslides [e.g., *Sutherland et al*., 2002], and forest felling [e.g., *Madej and Ozaki*, 1996; *Kondolf et al*., 2002], and also in rivers affected by volcanic eruptions in their headwaters [e.g., *Simon and Thorne*, 1996; *Montgomery et al*., 1999]. It is, however, possible for textural adjustment to allow a major addition of sediment to be evacuated rapidly without significant aggradation, as observed by *East et al*. [2015] following dam removal. The same range of responses has been observed in flume experiments, some of which have shown elements of wave-like behavior [*Lisle et al*., 1997; *Cui et al*., 2003; *Madej et al*., 2009], whereas in others an increase in supply has been accommodated primarily by textural adjustment of the bed [*Sklar et al*., 2009; *Venditti et al*., 2010a, 2010b]. The likelihood of significant aggradation increases with the volume of added load relative to the power of the river and the caliber of added load relative to the preexisting bed sediment and is higher with sudden point additions (potentially blocking the channel) than with more dispersed additions [*Cui et al*., 2005; *Lisle*, 2008].

In this paper we use numerical modeling to reconstruct the effects of a massive addition of sediment to Fraser River in British Columbia, Canada, as a result of placer mining for gold. Mining along Fraser River began as a gold rush in 1858 near Yale (Figure 1), close to where the river emerges from a canyon between the Coast and Cascade Mountains, and subsequently extended a short way downstream and almost 500 km upstream [*British Columbia Department of Mines*, 1946; *Nelson*, 2011]. The volume and caliber of sediment excavated by mining on the terraces alongside the river have been reconstructed by *Nelson and Church* [2012], who identified 453 separate mines and estimated that a total of 58×10^6 m^3

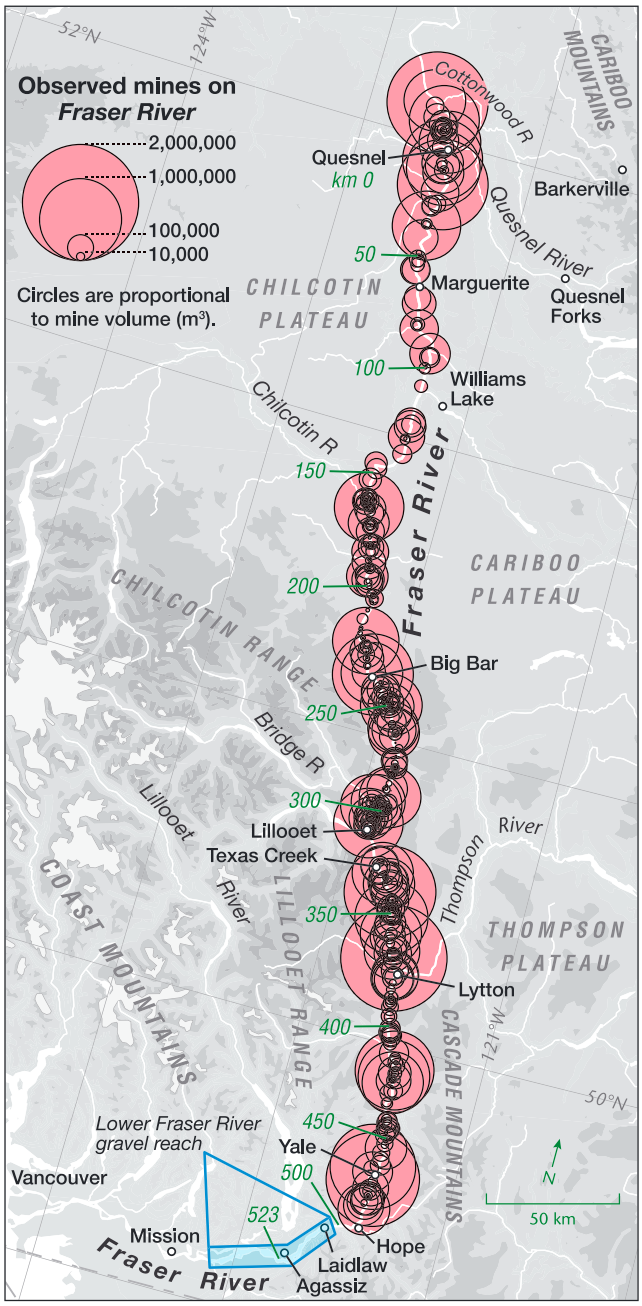

Figure 1. The middle and lower reaches of Fraser River, with sites of 1858–1909 gold mining. The "Lower Fraser Valley" is the lowland corridor from Hope to Vancouver. Distances in the study domain are marked in 50 km increments. The riverbed gravel-sand transition is at the downstream limit of the marked "gravel reach."

(bulk volume) of excavated sediment was washed into the river between 1858 and the end of commercial mining in 1909. We show later that this averages out to several times the likely natural load of the river, but it was distributed over a greater distance and time than in any of the case studies cited above and was added to a much larger river—the second biggest of all those draining to the Pacific coast of North America. Increased flood risk from aggradation is a key management concern along the distal course of the river in the heavily settled Lower Fraser Valley of British Columbia [*Church et al.*, 2001], so whether mining generated a significant sediment wave beyond the mountain front, and if so the timing of its passage, is of considerable practical importance. *Nelson and Church* [2012] suggested that while the peak delivery of placer waste past Hope probably occurred early in the twentieth century, the tail of a wave may still be present. This conclusion was reached by calculations in which the space-time distribution of tailings supply was staged along the river at three alternative constant sediment velocities which were extrapolated from tracer pebble studies in small rivers.

Here we investigate the effects of gold mining on Fraser River more thoroughly by using a physics-based morphodynamic model to simulate the entire transient response of the river to the added sediment load. The model is essentially the same as those developed and applied in previous work by ourselves [*Hoey and Ferguson*, 1994; *Ferguson and Church*, 2009], other researchers [e.g., *Cui et al.*, 1996; *Cui and Parker*, 2005], and agencies and consultancies (for example, the HEC-RAS code). The main novelty lies in overcoming two challenges: the premining state of the river is unknown and there is very little information about modern conditions along most of the river with which to tune the model's process representation or test the results. If a morphodynamic model is used to predict the response to some planned disturbance, for example, dam removal, fieldwork can be done to quantify the initial state and the details of the model can be tuned or "zeroed" [*Cui et al.*, 2006] to give initial quasi-equilibrium. But there is no information about what the middle course of Fraser River was like in the 1850s or how much bed load it conveyed, and hardly any modern information with which to zero a model, so we have had to devise a way of assessing the impact of gold mining on the river despite uncertainty

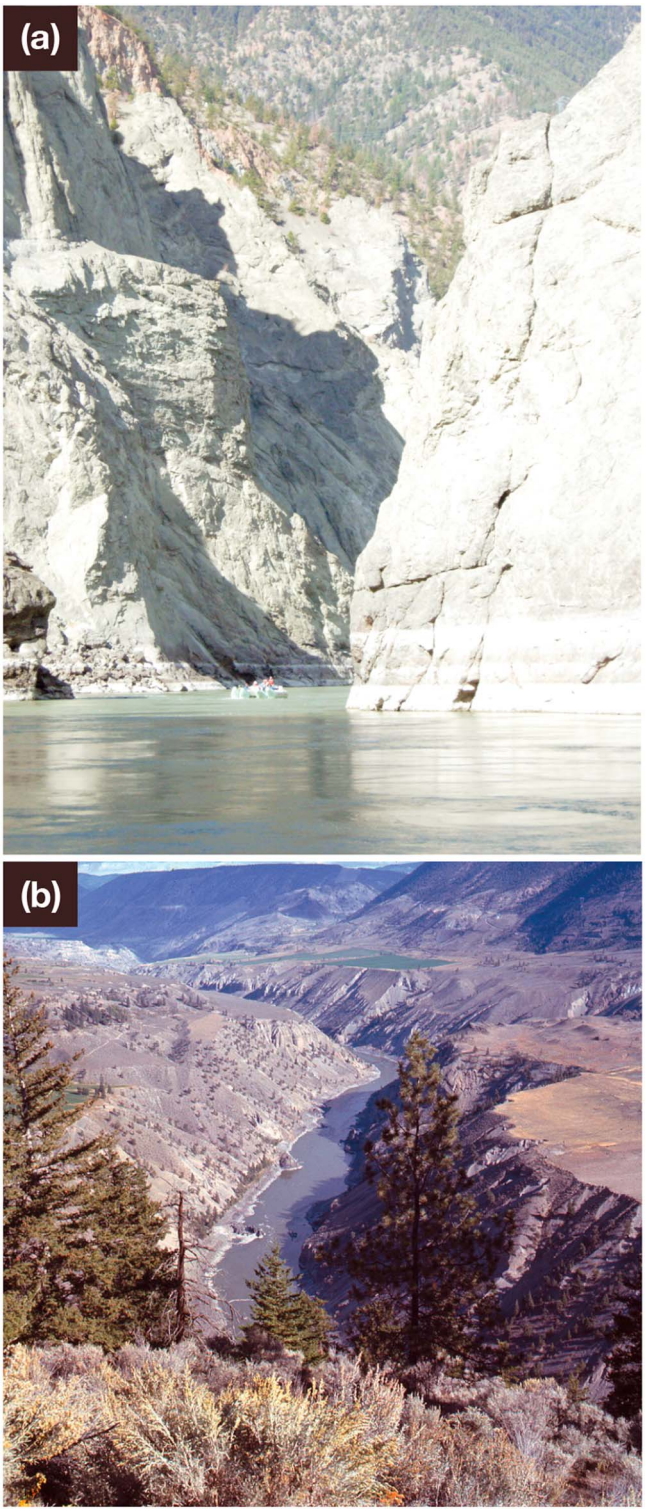

Figure 2. Typical examples of confinement of middle Fraser River by (a) rock (White Canyon, km 289) and (b) Pleistocene valley fills (near model km 292). Photos by M.C.

about the initial and boundary conditions and some auxiliary assumptions in the model. Our strategy differs from the "zeroing" of *Cui et al*. [2006] and may be useful in other investigations of past or present-day disturbance to rivers about which quantitative information is sparse. The paper is also the first investigation of how a large gravel bed river responds to supply change, and the results have implications for the future management of lower Fraser River.

2. Geomorphology and Hydrology of Middle Fraser River

Fraser River drains about 230,000 km^2 of southern and central British Columbia. It rises in the Rocky Mountains, traverses the Interior Plateau until 88 km past the town of Quesnel, then flows between the Coast Mountains and Cascade Mountains in a 370 km long series of canyons (known collectively as "Fraser Canyon") before emerging at Laidlaw onto a narrow floodplain which extends for 160 km to the outer edge of the river's delta (Figure 1). Lower Fraser River (downstream from the mountain front) and the upper part of the river in the Interior Plateau are unconfined with many gravel bars exposed at low flow and a few vegetated islands, but in Fraser Canyon the river is almost entirely confined by Pleistocene valley fill deposits or mountain sides, with rock walls along 18% of the distance and 42 separate deep, narrow rock canyons [*Venditti et al*., 2014]. Figure 2 shows typical examples of confinement by rock and valley fill. Unconfined reaches have a cobble/gravel bed with some marginal and subsurface sand, and the river continues to have a predominantly gravel bed until 58 km past the mountain front where there is an abrupt gravel-sand transition [*Venditti and Church*, 2014]. Bed character in the canyons is unknown in detail, but there is typically an alluvial channel that grades to a planar bedrock channel at the entrance to each canyon and a deeply scoured pool within the canyon [*Venditti et al*., 2014]. Longer canyons have several successive deep pools. There are boulder rapids

and exposed rock shelves in places, and the deepest parts of the channel probably have a transient cover of boulders and cobbles. There are no obvious signs of systematic aggradation or degradation in the Interior Plateau or Fraser Canyon, but the lower Fraser River gravel reach is known to be aggrading in many places.

The hydrological regime is dominated by seasonal snowmelt in the mountains and Interior Plateau. At Hope, where there is a continuous discharge record from 1912, the mean annual flood is 8640 $m^3 s^{-1}$ with no obvious trend over time in annual maxima. There are shorter records from four other sites on the main river (Quesnel, Marguerite, Texas Creek, and Agassiz; Figure 1) and six on tributaries, of which the biggest by far is Thompson River. The contributions from the various plateau subcatchments are almost in phase, but two west bank tributaries draining the Coast Mountains peak later than the Fraser itself and the other tributaries.

There is far less information about the geomorphology of this part of Fraser River than about its hydrology. Research on lower Fraser River by *McLean et al*. [1999], *McLean and Church* [1999], *Church et al*. [2001], and *Rice and Church* [2010] included measurements of channel change and bed grain size distributions (GSDs) in the unconfined distal reach and offered estimates of the gravel flux leaving the mountains both by analysis of bed load measurements made by the Water Survey of Canada at Agassiz in 1966–1986 and by construction of 1952–1984 and 1952–1999 sediment budgets from repeat surveys. But before this modeling project began, no survey or other data existed for the river channel within the mining region apart from cross-section surveys at the gauging stations, scour analysis at Marguerite [*Hickin*, 1995], and one GSD from a bar near Lillooet [*Ryder and Church*, 1986].

3. Methods: Morphodynamic Model and Boundary Conditions

The model is a 1-D (width-averaged) representation of flow, bed material transport, and transient channel adjustment from 1858 onward at nodes 1 km apart, starting at Quesnel in the Interior Plateau (model km 0) and ending at Agassiz (km 522) which is at the start of what in recent decades has been the most rapidly aggrading part of lower Fraser River. The use of a 1-D approach is forced by the lack of sufficient survey data to set up a 2-D or 3-D model, quite apart from considerations of computer power. *Cui et al*. [2008] showed that a 1-D model simulated sediment transport through a pool-riffle channel more accurately when the irregular along-reach variation in channel width and bed elevation was strongly smoothed, and we take the same approach here since our primary interest is in the amount and timing of gravel export from the mining region, rather than local details.

3.1. Channel Width

River distances and channel widths were obtained by measurements at 0.5 km intervals along the river center line on Google Earth imagery. Steep channel margins could usually be identified, in which case the width was measured between them; elsewhere, vegetation limits were used. Vegetated islands and large rock islands were excluded but not gravel bars that would be submerged at high flow. The midpoints of every second width transect are used as nodes in the model. Lack of information forces the assumption that channel widths have not changed significantly over the model time period. This is probably correct for the ~400 km along which the channel is deeply incised and confined by high talus slopes or rock. In the unconfined alluvial reaches mining-induced aggradation may have led to temporary widening with subsequent degradation and narrowing, but there is no archival or geomorphological evidence of significant changes. The Google Earth widths vary greatly, from 42 m in one rock canyon to maxima of 640 m and 1027 m in the proximal and distal alluvial reaches. The extremes reflect local peculiarities (rock constrictions and division around medial bars) which are subgrid scale for purposes of our model, so the width series was smoothed using locally weighted scatterplot smoothing (LOWESS) [*Cleveland*, 1979]; this also suppresses any sensitivity of model results to errors in individual widths. A 40 km window width sufficed to eliminate local irregularities while retaining all the main multikilometer expansions and contractions in width. This raised the minimum width to 95 m and reduced the maximum proximal and distal widths to 422 m and 497 m. The latter figure is close to the modern width at Agassiz.

3.2. Longitudinal Profile

Morphodynamic modeling requires knowledge of the initial longitudinal profile of the river bed. As discussed below (section 4), this is unknown in the present case and had to be estimated from knowledge of the modern profile. This too was unknown until we made measurements during a raft traverse from Quesnel to below Agassiz in 2009 [see *Venditti et al.*, 2014]. Water depth was measured by echo sounder, center line velocity profile by acoustic Doppler current profiler (ADCP), and raft location and water surface elevation by differential Global Positioning System, all at intervals of ~1 s which corresponds to every few meters depending on raft speed. The data comprise over 150,000 locations but with gaps where the instruments were portaged past a major rapid or the GPS signal was lost in deep canyons. The raft track contains loops and deviations for landings, so its cumulative length exceeds the Google Earth distance. The two series were reconciled by identifying the closest raft GPS position to each model node, deleting landings and zigzags and rescaling the cumulative raft distance. To minimize the influence of gaps and discontinuities, we took the median depth around each model node and used a variable-width Gaussian-weighted moving average of the surface elevation series to remove negative water surface slopes. Depths measured from the raft generally refer to the talweg, so subtracting them from the water surface elevation would give too low a mean bed elevation unless sections were rectangular everywhere, which seems unlikely. Instead, we assumed parabolic sections (in which, by integration, the mean depth is two thirds of the maximum depth irrespective of aspect ratio) and estimated the mean bed elevation at each node accordingly. Despite the smoothing of the raw data, the resulting bed profile is irregular, with elevation differences ranging from -12 to 14 m km^{-1}.

3.3. Model Structure

Simulations proceed by iterative numerical calculation using time steps of the order of 1 day. In each step the water surface slope (S), mean depth (d), mean velocity (v), and bed shear stress at each node are computed using the St. Venant equations for gradually varied flow. Transport rates of 13 size classes of bed material ranging from coarse sand to boulders are calculated using the local bed grain size distribution (GSD) and shear stress. The longitudinal profile and bed GSDs are then updated using discretized versions of the Exner equation for conservation of total sediment mass

$$\partial z/\partial t = -(\partial Q_T/\partial x)/((1-\lambda)w) \tag{1}$$

and the fractional Exner equations

$$\partial F_i/\partial t = (E_i \partial Q_T/\partial x - \partial Q_i/\partial x)/((1-\lambda)wL) \tag{2}$$

for conservation of mass of each size class $i = 1$ to 13 in an active layer of thickness L. In these equations x is distance downstream, t is time, Q_T is total bed material transport rate (volume per unit time), w is channel width, λ is bed porosity, F_i is the proportion of size class i in the active layer, Q_i is the transport rate of this size class, and E_i is the proportion of class i in the material exchanged at the base of the active layer. The $\partial Q/\partial x$ terms in these equations take account of any lateral inputs of sediment from tributaries, sidewall mass movement, or mining waste.

Simulations have to start from some assumed initial state, which we discuss later. They also require specification of several boundary conditions and auxiliary assumptions. The necessary boundary conditions are the water discharge at each node and time, the spatial and temporal pattern of bed material supply to the river, the flow depth at the distal node, and the substrate GSD in the event of bed lowering. Required auxiliary assumptions are a flow resistance equation, a bed load transport equation, the minimum grain size considered in the model, and details of the active layer scheme and porosity.

3.4. Hydrology

Computations are made for a steady dominant discharge operating for a small proportion of the time, with the time derivatives in the Exner equations adjusted accordingly as in *Parker* [2004]. *Ferguson and Church* [2009] found when modeling lower Fraser River that simulations using a 20 year hydrograph with annual peaks ranging from 6070 to 12900 m^3 s^{-1} generated substantial year-to-year variation in locations and amounts of aggradation and degradation; however, net changes over 20 years were matched quite closely by a model using a steady dominant discharge of 7000 m^3 s^{-1} operating for 15% of the time. This pair of discharge and intermittency values was the unique combination that predicted not only the same total

flux as the 20 year hydrograph but also the same overall bed load GSD. We retained this approximation of the hydrological regime at Agassiz for our mine waste simulations and used the fact that 7000 $m^3 s^{-1}$ is 82% of the median annual flood at Agassiz to estimate dominant discharges at the other gauging stations. Comparison of the estimates for the main stem gauging stations at Marguerite, Texas Creek, Hope, and Agassiz with the sum of the inflows upstream from them showed close agreement at Marguerite but differences of up to 6% at the others. Exact agreement at Agassiz, and agreement to within 1% at all other stations, was achieved by reducing the assumed inflows from the two out-of-phase Coast Mountain tributaries and adding a small (2 $m^3 s^{-1} km^{-1}$) lateral inflow along the last 200 km of the river to account for minor tributaries draining the more humid mountains. The model domain begins at the confluence of Quesnel River whose discharge is combined with that of the Fraser immediately upstream as a single inflow of 3730 $m^3 s^{-1}$.

3.5. Flow Calculations

The St. Venant equations are solved using a predictor-corrector step-backwater scheme which is second-order accurate. The friction slope is defined by the Darcy-Weisbach resistance law $v^2 = 8gdS/f$, and the depth at Agassiz is calculated for uniform flow. Possible specifications of the friction factor f include a spatially and temporally varying value according to relative roughness, a fixed value of Manning's n (implying $f \propto d^{-1/3}$), or a fixed value of f. Field information to guide the decision is scarce and contradictory. At each hydrometric station f decreases as Q increases, but none of the popular flow resistance laws fits all the stations well. Mean depths and velocities derived from ADCP transects made during the 2009 raft trip (see *Venditti et al*. [2014] for details) imply higher f values in deeper sections, which is inconsistent with the at-a-station trends and with standard resistance equations. We therefore resorted to a fixed value of $f = 0.048$ at all nodes, this being the median of the dominant discharge f values at the hydrometric stations. Using a higher friction factor in canyon sections would increase total shear stress, but it is likely that much of the total stress is expended on sidewall resistance and not available for bed load transport. The simulated amount and timing of tailings export is not very sensitive to the specification of f; for example, increasing f by 17% everywhere gives only a 5% increase in mean shear stress and only 4% more bed load passing Hope and Agassiz.

3.6. Bed Load Transport

Bed GSDs in the model quantify the proportion by weight in 13 size classes: 0.5–2 mm coarse sand, four whole-phi gravel fractions from 2 to 32 mm, and eight half-phi gravel, cobble, and boulder fractions from 32 to 512 mm. Wider classes (in terms of phi) in the fine tail of the GSD are justified because the differences in reference shear stress (in N m^{-2}) are smaller. Transport rates of each class are calculated using the equations of *Wilcock and Crowe* [2003]. Neither these nor the main alternative [*Parker*, 1990] were calibrated on such coarse sediment as in parts of Fraser River, but both give good fits to the measured bed load rating curve at Agassiz [see *Ferguson and Church*, 2009], and the Wilcock-Crowe equations have the advantage of allowing for greater gravel mobility when there is a high proportion of sand in the bed, as might be the case during mining. The 0.5 mm minimum grain size was chosen after calculating what sizes would travel almost entirely in suspension in different parts of the river, using the *Dade and Friend* [1998] criterion $w_s/u^* < 0.3$ (where w_s is settling velocity and u^* is shear velocity) and the *Ferguson and Church* [2004] equation for w_s. This showed that 0.25 mm sand moves in continuous suspension at all nodes, and 0.5 mm sand at more than 400 nodes, but 1 mm sand at only 16 nodes. The 0.5–1 mm fraction therefore has to be included in the model, even though in reality it will be suspended at the narrowest sections, but the 0.25–0.5 mm fraction is largely irrelevant. Abrasion is neglected since *Cui and Parker* [2005] found that its effects on pulse behavior were negligible unless grains are reduced to half their diameter in less than ~100 km. This is implausible in Fraser River where lithologies are mostly resistant igneous and metamorphic types that have survived glacial cycles.

3.7. Active Layer

Updating bed elevation and GSD using equations (1) and (2) requires assumptions about bed porosity, active layer thickness, and exchange material GSD. We used $\lambda = 0.3$ and $L = 3D_m$ (where D_m is the geometric mean bed diameter) and assumed that during aggradation, deposited gravel is mixed entirely into the active layer but half of the deposited sand passes to the substrate. A slightly

higher/lower porosity value gives slightly more/less change in bed elevation but with little effect on shear stress or bed load transport. Sensitivity tests showed that higher or lower L/D_m and less or more sand infiltration only affected the rapidity of grain size change in the first year or so after the onset of mining and had no perceptible effect on the longer-term sediment budget. During degradation E_i is equated with the current active layer GSD when and where the bed is above its premining level, otherwise with the premining GSD. Based on observations of rock walls, rock shelves, and boulder rapids during the 2009 raft trip, we also set a rock floor 0.1 m below initial bed level at 10 nodes and 1 m below it at another 150 nodes. If the river reaches this floor, the sediment flux and its GSD are set equal to those at the next node upstream so that incision is prevented. In typical simulations the rock floor is reached in four short reaches, all known to be rock canyons.

3.8. Sediment Supply

A key boundary condition is the natural supply of sediment >0.5 mm in diameter to the river each year at each node. The results presented below assume that bed material load is supplied only by inflowing water (Fraser River plus Quesnel River at km 0 and the five tributaries included in the model) and that the supply rate is steady over time. The cumulative natural supply therefore increases in steps at tributary junctions but is constant between junctions. The GSD of the supply at km 0 is set to match the transport capacity for each size fraction at that node, as calculated from the shear stress and bed GSD. No bed load measurements have been made on any of the tributaries nor are data available on tributary bed GSDs and gradients from which to calculate the amount and caliber of load from each tributary. For lack of better information we assume that tributaries contribute load in proportion to their water discharges and with the same load GSD as at the km 0 inflow. We tested two other scenarios for the spatial pattern of supply: one in which significant amounts of sediment are added by slope processes in the confined reaches and one in which the contribution from Thompson River is far less than proportional to its discharge because it drains a major lake and has a rock/boulder bed. Neither made any significant difference to model results, because the procedure described below for determining premining bed GSDs compensates for changes to the pattern of supply.

The sum of the six inputs defines the total natural bed load supply (TNS). In equilibrium this would also be the bed load flux at Agassiz, but it could be lower than the modern flux at Agassiz if a mining-induced sediment wave is still passing that location or higher if the mining effect is already complete and there is some natural aggradation above Agassiz. Moreover, the modern flux at Agassiz is itself uncertain. *McLean et al.* [1999] estimated an annual gravel load of 0.23 million tonnes (Mt hereafter) by fitting a rating curve to the 1966–1986 measurements, and *McLean and Church* [1999] obtained a similar estimate from their 1952–1984 sediment budget, but *Ferguson and Church* [2009] showed that the 1966–1986 measurements were equally consistent with a mean gravel flux of 0.39 Mt yr^{-1} which was the central estimate from the 1952–1999 sediment budget. *Church et al.* [2001] and *Nelson and Church* [2012] suggest a likely annual flux of 0.3–0.4 Mt yr^{-1}. The full range of possibilities was covered by running simulations with TNS = 0.2, 0.3, 0.4, and 0.5 Mt yr^{-1}. TNS in the model includes all sizes from 0.5 to 512 mm; the 2–512 mm ("gravel" hereafter) supply is 0.18, 0.28, 0.37, or 0.47 Mt yr^{-1}.

In mining runs the natural supply is augmented by tailings, distributed over time and along the river in accordance with the reconstructions of *Nelson* [2011, Figure 2.3 and Table C1]. The temporal pattern is known only at regional scale, from a requirement for mine owners to declare the value of gold production. It shows two main peaks of activity around 1860 and 1900. It is likely that mines farther up river were relatively more important in the second peak, but the data are insufficient to allow for this in our simulations. By sampling sediment in former mining areas, Nelson constructed an "average tailings" GSD. It extends to 128 mm and contains 35% of sand and silt finer than 0.5 mm. Converting from bulk volume to sediment mass using a porosity of 0.3 and sediment density of 2650 kg m^{-3}, the total tailings input to the river is 108 Mt. The input coarser than 0.5 mm amounts to 70 Mt, with D_m = 10 mm and containing 20% of coarse sand. An even larger volume of material was excavated in mines close to the upper reaches of Quesnel River and two smaller east bank tributaries which join Fraser River approximately 30 km and 150 km upstream of Quesnel. Our simulations exclude these sources since they are mostly 50–100 km up the tributaries and field observations indicate that much or most of that material remains sequestered within the tributary stream systems, which have aggraded by >10 m in places [*Galois*, 1970].

4. Methods: Defining the Initial System State

The premining longitudinal profile and bed GSDs are unknown. Defining them proved to be the biggest challenge in the historical reconstruction reported here. It is also likely to be a problem when modeling present-day disturbances to rivers in remote areas where there are few or no grain size data, so our approach may be more widely useful.

Our original plan was to generate a premining state by running the model from some long-ago state until a quasi-equilibrium was reached in which the longitudinal profile broadly resembled the raft traverse profile and local aggradation or degradation did not exceed 1 mm yr^{-1}. This "spin-up" procedure was used by *Ferguson and Church* [2009] when modeling 38 km of lower Fraser River extending downstream from Agassiz and is functionally equivalent to the zeroing or "priming" of some other authors [*Cui et al*., 2006, 2008; *Viparelli et al*., 2011], but it failed here despite many attempts using different original profiles and GSDs. Reaching quasi-equilibrium along nearly all of the river required continuing the computations for ~2000 years, by which time the main convexities and concavities in the longitudinal profile had experienced ≥10 m of degradation and aggradation respectively so that the final profile was much straighter than the modern one. By implication, either our process representation or our boundary conditions (hydrology and sediment supply) are inadequate [*Cui et al*., 2008]; we could not, however, rectify this by zeroing [*Cui et al*., 2006, 2008] since that relies on good knowledge of bed GSDs and then involves making minor adjustments to the initial profile until quasi-equilibrium is achieved. In the present case the initial GSDs had to be guessed, and starting with accommodation space in the zones which aggraded the most merely made them aggrade faster. Moreover, even after such a long spin-up, the final 40 km or so in the model was still aggrading by a few millimeters per year.

Our solution to this impasse was to make the premining longitudinal profile a smoothed version of the modern one and create premining bed GSDs such that the transport capacity at each node matched the assumed cumulative supply of sediment from upstream. Starting from the modern longitudinal profile can be justified on the grounds that the many rock/boulder rapids are unlikely to have changed significantly since the 1850s, and they constrain the rest of the profile. We smoothed the raft traverse profile using LOWESS with a 25 km window. The root-mean-square difference between the LOWESS and raft traverse profiles is only 2 m, but the smoothing eliminated negative bed slopes, reduced the maximum bed slope from 14 m km^{-1} to 2.3 m km^{-1}, and gave the correct slope at Agassiz.

For the LOWESS longitudinal profile to be in equilibrium, the bed load transport rate at each node must equal the total natural sediment supply from all sources upstream from that node. To achieve this, we created premining bed GSDs by node-by-node optimization of a generic probability distribution with an adjustable parameter that makes the bed coarser or finer. An obvious possibility is the lognormal distribution with fixed phi standard deviation and optimized phi mean, but the few available modern GSDs from relevant parts of the river are asymmetric on the phi scale, with the fine tail longer than the coarse tail. An alternative which possesses this characteristic is the Rosin distribution, which was first proposed for crushed coal [*Rosin and Rammler*, 1933] but also fits river bed and bed load GSDs [*Ibbeken*, 1983; *Shih and Komar*, 1990]. Its cumulative distribution function is

$$F(\leq D) = \exp[-(D/k)^s] \tag{3}$$

where k is the mode of the GSD and s an inverse measure of spread. The grain diameter D takes all positive values in (3), so for present purposes the <0.5 mm and >512 mm tails must be deleted and the distribution rescaled. *Shih and Komar* [1990] found that best fit values of s for the bed surface, subsurface, and high-flow bed load at Oak Creek were in the range 0.8–1.5; on this basis we used $s = 1.2$ as the fixed parameter in the distribution and optimized k node by node to give the desired transport rate. The GSDs optimized in this way vary greatly along the river in accordance with the variation in simulated shear stress (Figure 3) and are systematically coarser for lower natural supply rates. The geometric mean diameter ranges from a minimum of 23–29 mm (according to TNS) in the unconfined proximal and distal reaches to maxima of >200 mm in the narrowest and steepest canyons.

While matching capacity with supply at each node is a necessary condition for equilibrium, giving $\partial z/\partial t = 0$ in the Exner equation, it is not a sufficient condition. This is because the combination of size-selective transport with downstream variation in GSD implies nonzero gradients in the transport rates of individual size fractions

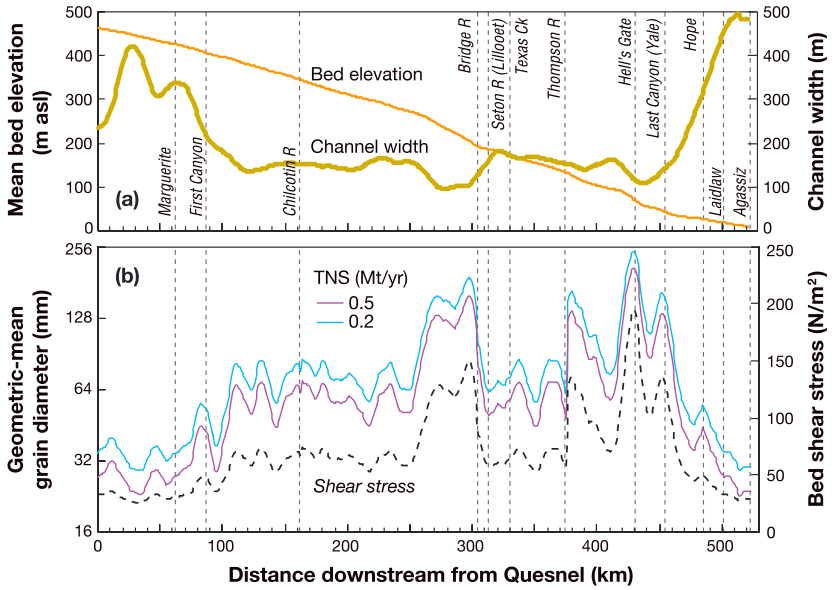

Figure 3. Premining initial state of the model: (a) longitudinal profile and channel width and (b) geometric mean bed grain diameter for the highest and lowest estimates of total natural bed load supply (TNS). Downstream variation in shear stress is also shown. Principal places mentioned in the text are superimposed.

($\partial Q_i/\partial x \neq 0$ in equation (2)). This causes changes in bed GSDs ($\partial F_i/\partial t \neq 0$ in equation (2)) and thus imbalances in transport capacity, leading to local aggradation or degradation. A recent mathematical analysis of the Exner, fractional Exner, and St. Venant equations [*Stecca et al.*, 2014] discusses this in terms of the so-called sorting waves which propagate rapidly downstream. Starting the model with the optimized GSDs therefore triggers transient changes which, although small, do not die out completely within the model time frame.

The fact that the initial state is not a perfect equilibrium led us to run two simulations for each scenario of natural sediment supply: a control run with no mine waste to establish the magnitude and location of the sorting wave changes and a mining run in which mine waste is added to the river during the first 52 years (1858–1909) but not subsequently. The predicted characteristics of the river toward the end of the mining run can be directly compared with available modern field data in the lowermost reach as a test of the veracity of the model's process representation and supply scenario, and the simulated behavior during the mining period throws light on how the river may have responded to increased sediment supply.

Determining how much sediment was delivered to lower Fraser River is less straightforward because it depends on the interpretation placed on the control run. Upper and lower bounds can be obtained from two end-member interpretations. In the unlikely event that the model and its initialization are perfect, the control run simply shows what the river would have done without mining, and the mining run is the best estimate of actual river behavior. The other, more plausible, extreme is that the premining river was actually in equilibrium and changes during the control run are entirely due to deficiencies in the model and/or its initialization. If so, they should be subtracted from the mining run to obtain a corrected estimate of actual river behavior. We return repeatedly to this dilemma in the rest of the paper and allow for the uncertainty by presenting results for the two extreme cases.

5. Simulation Results

We begin by summarizing what happens in control runs then describe in more detail what happens during mining runs and what the simulations say about the delivery of gravel from the mining region to lower Fraser River. Some results are illustrated up to the present time (2015), but others are truncated in 1999 which is the end of the period for which empirical estimates of gravel flux at Agassiz exist.

5.1. Changes During Control Runs

The sorting wave adjustments have no net effect on the model longitudinal profile. Local erosion is almost exactly canceled by local aggradation, with no more than ±2 Mt of sediment gain or loss in the system at any time in simulations with any of the four supply scenarios; that corresponds to a change in mean bed level of only ±0.01 m. The amplitude of local changes increases slightly with the total supply rate but remains less than ±0.5 m at 75–85% of model nodes including the whole of the first 250 km of the river. To put this in context, annual scour and fill at the gauging stations can approach 2 m [*Hickin*, 1995]. The biggest changes occur in the same places in each control run: erosion down to the rock floor in canyons around km 290 and 425, aggradation at profile concavities 10–20 km downstream from these (to a maximum of 2.1–2.8 m at km 305), erosion immediately past the confluence of Thompson River where river discharge increases by 50%, and aggradation of up to ~2 m at km 460–470 (south of Yale) where the channel becomes wider and less steep. In each case the simulated behavior is qualitatively plausible as a natural tendency, but the rates of change (locally more than 10 mm yr^{-1}) are higher than expected in a river that has had thousands of years since deglaciation in which to approach equilibrium. This suggests that the control run changes are at least partly, and probably mainly, due to deficiencies in the model. In particular, the validity of our flow resistance and transport rate calculations in the steepest and narrowest canyons is doubtful in view of the 3-D flow structures described by *Venditti et al.* [2014]. Overestimation of effective shear stress and transport capacity here would necessarily lead to overestimation of aggradation where capacity decreases a little farther downstream.

5.2. Aggradation During Mining Runs

The results of mining simulations with different natural supply scenarios differ only slightly. This is not surprising because the average rate of >0.5 mm tailings supply (1.4 Mt yr^{-1}) greatly exceeds the assumed TNS of 0.2–0.5 Mt yr^{-1}. In each run there is net aggradation in and beyond the reach directly affected by mining, but the mean aggradation is only ~0.1 m and many nodes degrade rather than aggrade. The simulations show little evidence of topographic wave propagation. Aggradation profiles at three stages in the simulation with TNS 0.4 Mt yr^{-1} are shown in Figure 4a. Aggradation is not strongly correlated with tailings inputs: some of the main aggradation zones (e.g., km 0–30) are a short way downstream from mining hot spots, but others are not. The main locations of deposition and erosion are fixed after the first few years of mining, and the amplitude of change at these locations increases throughout the rest of the mining period. The maximum aggradation depth in each mining run (2.5–2.8 m depending on TNS) is little or no higher than in the corresponding control run and is located in the same place, and other loci of significant erosion and deposition also coincide (Figure 4b). Because of this, the typical amplitude of change in mining runs is much less if control runs are interpreted as model error and elevation changes during them are subtracted from changes in the mining runs. The root-mean-square difference in elevation between mining and control runs by 1999 is only 0.2–0.3 m (depending on TNS), compared to a root-mean-square difference of 0.6–0.7 m between the mining run profile at that date and the premining profile.

The temporal pattern of aggradation during mining is illustrated in Figure 5 by time profiles of the amount of gravel (by which we mean all sizes from 2 to 512 mm) added to storage between Quesnel (km 0) and the mountain front at Laidlaw (km 500) since the start of mining. We show gravel results because the field data on bed load transport down river from Laidlaw are for >2 mm sediment. Profiles of total storage including coarse sand are very similar in shape but 10–20% higher. The pattern is the same for each TNS scenario and reflects the variation over time in mining activity: aggradation at times when the pace of mining was increasing (1858–1860, early 1880s, and late 1890s) and degradation when it was decreasing and for several years after it ceased. The rapid decrease in storage after each peak implies a short residence time for much of the added sediment. The first peak in storage represents almost all of the tailings added in the first 3 years of mining, but the second peak is equivalent to only ~30% of the cumulative tailings input to 1900, implying that most of the extra sediment has already been transported out of the mountains. The loss of gravel from the system continues for 5–15 years after the end of mining in 1909, indicating that the addition of tailings had increased gravel fluxes to above the natural rate of supply, but subsequently, the balance tips the other way with gradual accumulation. Correcting the curves

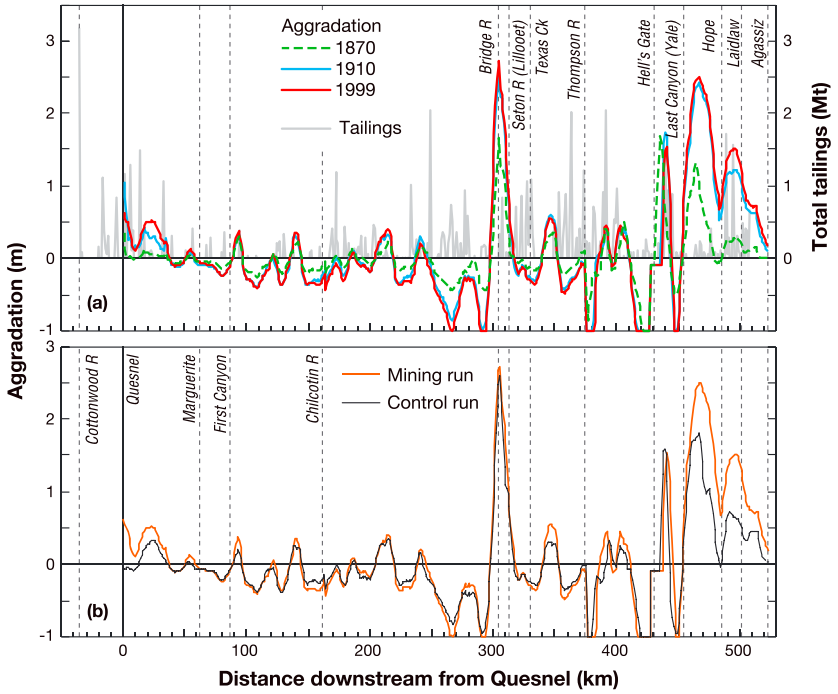

Figure 4. Simulated distribution of aggradation during and after mining with total natural bed load supply (TNS) set as 0.4 Mt yr^{-1}. (a) Evolution of bed elevation in mining run, with distribution of tailings inputs along the river overlaid in gray. (b) Compares the 1999 situation in mining and control runs. Mining inputs upstream from Quesnel are added to the supply to km 0 in the model.

for changes during the corresponding control runs makes very little difference since, as already noted, the maximum change in storage during control runs was less than 2 Mt.

5.3. Bed Load Transport During Mining Runs

For storage to adsorb relatively little of the total supply of tailings, bed load transport rates out of the mining area have to be high. Figure 6 shows the simulated downstream variation in gravel flux at various times during and after the mining period. The effect of switching mining on is to increase fluxes dramatically. For the first few years, including the first peak of mining activity in 1860, there are large downstream variations in transport rate. This is indicative of separate bed load pulses, but few of the peaks coincide with mining hot spots. By 1861 pulse fronts are apparent near km 90, km 310, and km 520. The first of these must relate mainly to tailings supply at or not far downstream from Quesnel, since mining activity was very low between km 40 and 120; the effects of mining therefore propagate ~50 km in 3 years. Similarly, the big increase in gravel flux at all nodes from the farthest downstream mine at km 480 to the pulse front near km 520 indicates a pulse celerity of at least 13 km yr^{-1}. These celerities are much higher than the sediment virtual velocities that *Nelson and Church* [2012] adopted in their calculations, though comparable to what *East et al.* [2015] observed following removal of a dam on a steep gravel bed river. By 1865 modeled transport rates as far as km 50 are back to premining levels in response to the decline in mining activity after the 1860 peak, but previously mobilized sediment continues to be transported at a high rate in the rest of the river. The cumulative effect of tailings additions now gives a near-continuous increase in gravel flux as far as km 460. Beyond that point the flux declines but remains

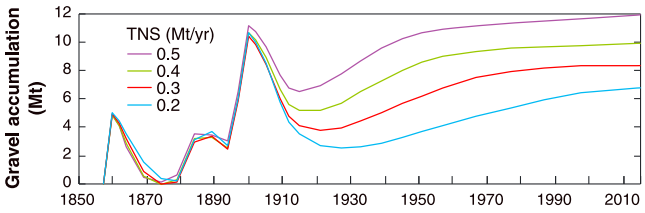

Figure 5. Time profiles of gravel storage between km 0 and km 500 since start of mining in simulations with different rates of total natural bed load supply (TNS).

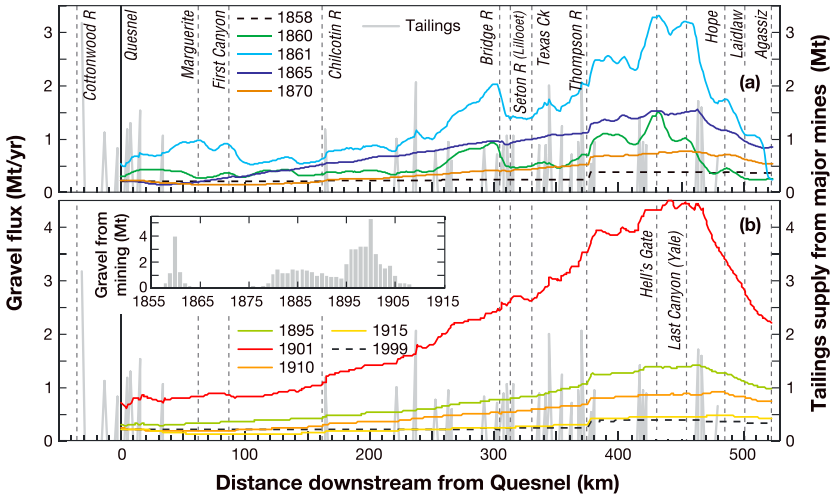

Figure 6. Profiles of gravel flux at different stages in a mining simulation with total natural supply 0.4 Mt yr^{-1}; (a) early mining peak and (b) late mining peak. In this and Figure 7 each profile is for the start of the indicated year. The spatial pattern of total tailings input is overlaid in gray, and its temporal distribution is shown in the inset.

extremely high compared to premining times; at Agassiz it is more than twice the initial value. This 1865 profile can be regarded as a single large sediment pulse, and the decline in flux toward and beyond the downstream end of mining activity implies aggradation in the final 60 km or so of the model domain.

Mining activity remained low for the next 15 years, so the 1870 flux profile is a scaled-down version of the one for 1865. By 1895 mining activity was rising toward its second peak and the flux profile closely resembles that for 1865. The second peak of mining activity in 1900 generated the highest fluxes of all (1901 curve), with a maximum of over 4 Mt yr^{-1} of gravel—10 times the premining rate. Mining declined after 1900 and became negligible after 1909, but the simulated flux profile at the start of 1910 retains the previous wave shape and reaches a maximum of twice the premining flux. Fluxes decline rapidly over the next few years, dropping slightly below premining values in many places, then increase very gradually. By 1999 the flux profile is very close to matching the assumed natural sediment supply from km 0 to about km 460 but falls slightly below it thereafter.

5.4. Fining and Coarsening of the River Bed

How can tailings disposal increase gravel flux so dramatically? The answer, according to our model, lies in fining of the river bed. We illustrate this in Figure 7 for a TNS of 0.4 Mt yr^{-1}; the equivalent plots for other natural supply rates are almost the same. By the start of 1861 (after the first peak in mining activity) the simulated geometric mean grain diameter is about 30% lower on average as far as the distal wavefront. This bed fining reduces the reference shear stress used in the bed load transport calculations, and the nonlinearity of the transport equations explains why a moderate decrease in D_m can increase transport rates by a much bigger factor. The effect is emphasized somewhat by our use of the *Wilcock and Crowe* [2003] transport equations but not by much because the sand content of the bed remains below 10% everywhere. By 1870, after several years of low mining activity, fining has extended past Agassiz but the bed has become coarser everywhere else. The bed is now slightly coarser than it was before mining in the first 150 km of the model domain, about the same for the next 150 km, but thereafter slightly finer. This implies preferential onward transport of fine sediment introduced in the first main phase of mining. A similar fining-then-coarsening cycle occurs as the tailings supply increases to the second peak in 1900 and then declines. The tailings supply in 1900 was greater than in the 1860 peak, and the simulated fining of the river bed at the start of 1901 is even more pronounced: a 44% average reduction in D_m and a peak sand content of 15%. The reduction exceeds 50% for most of the distal 200 km of the river, including Agassiz where the simulated geometric mean is 12 mm compared to 25 mm before mining began. But by the end of mining, just 9 years later (1910 curve in Figure 6), the bed has already returned to approximately its premining state, and by 1915 much of it is slightly coarser than before mining, in an

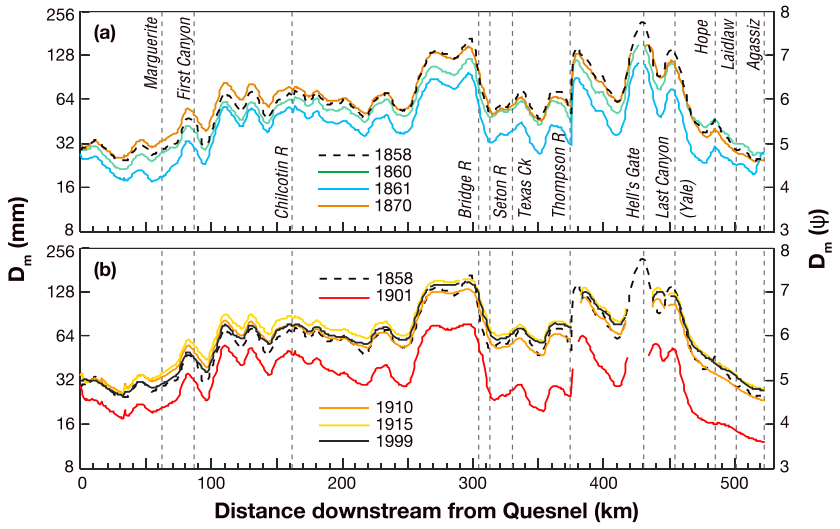

Figure 7. Fining and coarsening of the river bed during and after the mining period, as indicated by changes in geometric mean diameter during a simulation with total natural supply 0.4 Mt yr^{-1}; (a) early mining peak and (b) late mining peak. Gaps in the curves are where the river has eroded down to rock.

overshoot which implies that selective removal of available fine sediment from the reach temporarily exceeded replenishment from the natural supply. Thereafter the model simulates gradual and slight fining at almost all nodes as the overshoot is reversed, with 1999 bed GSDs which do not differ systematically from the optimized premining GSDs.

5.5. Gravel Delivery to Lower Fraser River

The total gravel supply to our model of Fraser River over the period from the end of 1857 to the start of 1999 comprises 56 Mt from mine tailings plus a natural load of 26–66 Mt (according to TNS scenario), making a total of 82–122 Mt. We have already seen in Figure 5 that relatively little of the total is stored within the mountains: 10–11 Mt by the end of the mining period and 6–11 Mt by 1999, according to TNS. But whereabouts between the mountain front and the gravel-sand transition is the other 90% or so deposited? Does it depend on the choice of natural supply scenario? And what if the control runs are interpreted as quantifying model error and are used to adjust the predictions of the mining runs?

Figure 8a shows simulated time profiles of gravel storage (relative to 1857) in the 22 km subreach from the start of the unconfined floodplain at Laidlaw to Agassiz, and of delivery past Agassiz, i.e., storage between Agassiz and the gravel front (a distance of 36 km at the present time). In these plots the steeper the curve, the faster the aggradation. The mining runs with different TNS scenarios all share several qualitative features. The most obvious one is that over the full simulation period, about three quarters of the gravel exported from the mountains also passes Agassiz: the cumulative volume of aggradation between Laidlaw and Agassiz is only about one third of that between Agassiz and the gravel front. The deposition of some 25–30 Mt of gravel downstream from Agassiz in the two decades from 1890 to 1910 must imply a substantial (several kilometers) advance of the gravel front and aggradation in the last few tens of kilometers above it. A second feature is that aggradation rates in both subreaches are higher for higher TNS, as would be expected. The third thing in common is the temporal pattern shown by all eight curves in Figure 8. Aggradation in both subreaches is rapid during and shortly after the first peak in mining activity (1860), continues more slowly through the 1870s when activity was low, picks up to a longer period of rapid aggradation around and after the second peak in mining activity in 1900, then declines drastically after the end of mining in 1909. After that, the simulated pattern of aggradation starts to differ between the two subreaches, with a gradual increase in the below-Agassiz aggradation rate but near equilibrium above Agassiz.

The aggradation profiles in Figure 8a are derived from the mining runs, with no consideration of the control runs. By implication they assume that changes in the control runs reflect a real disequilibrium in 1857, show

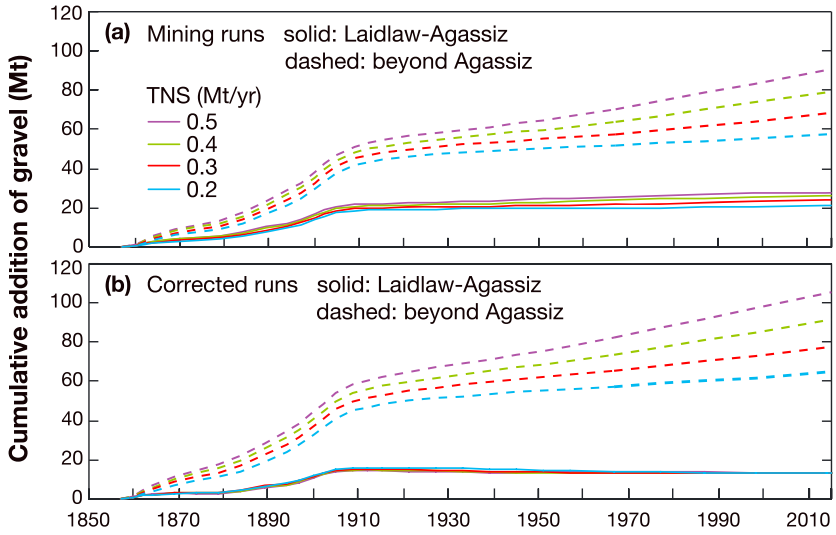

Figure 8. Simulated time profiles of gravel accumulation in mining runs with different rates of natural sediment supply (TNS). (a) Unadjusted results. (b) Adjusted for control run changes at each node. Separate curves are shown for accumulation between Laidlaw (km 500) and Agassiz (km 522) and from Agassiz to the gravel front.

how the river would have evolved in the absence of mining, and have nothing to do with imperfections in the model or its initialization. As discussed earlier it is possible to take the opposite view that the river was, in fact, in perfect equilibrium in 1857, but the model's initial state and process representation are imperfect and have caused spurious changes to occur in the control runs. In that interpretation, the best estimate of actual river behavior is to use the control run outcome to correct the mining run for model imperfections. This can be done by subtracting aggradation/degradation volumes in each 1 km cell in a control run from those in the corresponding mining run to generate a corrected aggradation profile as far as Agassiz. The difference between total input and total aggradation up river from Agassiz then gives a corrected estimate of gravel deposition below Agassiz. Time profiles adjusted in this way are shown in Figure 8b. They deviate progressively from the uncorrected mining run curves, showing (for any given TNS) even less overall aggradation between Laidlaw and Agassiz and even more beyond Agassiz. As in the uncorrected mining runs the gravel aggradation rate below Agassiz increases with TNS and increases over time after the 1940s, but the curves for the Laidlaw-Agassiz subreach are now almost the same for each TNS and show slight degradation for several decades after the end of mining and near equilibrium at the present day.

6. Discussion

6.1. Comparisons Between Model Predictions and Available Field Evidence

The simulated changes within the mining region and mining period are untestable except in one respect: *Nelson and Church* [2012] located historical photographs and written descriptions which strongly suggest that the middle course of the river did not experience major aggradation, in contrast to what was already known to be happening in streams draining the California gold rush area. Our prediction of only 0.1 m of aggradation on average is consistent with this archival evidence. Simulated aggradation was higher than this locally, as discussed above, but almost all of the nodes with 1 m or more of elevation change are in canyon reaches where a change in bed level might have no visible effect.

The main opportunity to test the model is in the lowermost part of the model domain where, as noted above, the gravel load has been estimated by rating curve and sediment budget methods and grain size distributions have been measured on bars exposed at low flow. The 1952–1999 sediment budget provides the most comprehensive test. It was derived from geographic information system calculations for 1 km long cells using repeated mapping of the river bed and banks and adjusting for officially authorized gravel extraction from bars and for the sand content of banks and bars. The surveys extended from the start of the unconfined reach at model km 500 (Laidlaw) to below the gravel front. The budget was first presented in *Church et al.* [2001], but here we use an unpublished 2008 update which quantified bank line retreat

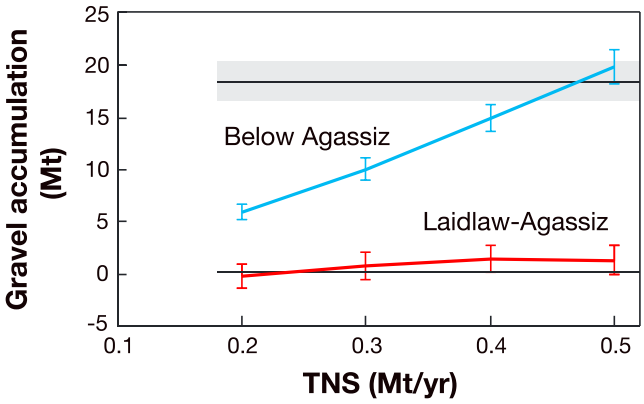

Figure 9. Comparison of 1952–1999 gravel accumulation in two parts of lower Fraser River as estimated from repeat surveys (horizontal lines) and as simulated by model (curves with error bars). Model predictions are shown for different scenarios of total natural sediment supply (TNS) and for mining runs uncorrected (upper end of error bar) and corrected (lower end of error bar) for changes during control run. Uncertainty in below-Agassiz sediment budget is shown by gray shading; uncertainty for Laidlaw-Agassiz budget is too small to be visible in this plot.

more accurately. There is considerable cell-to-cell variance in aggradation as a result of bar growth and associated bank erosion and talweg switching, processes which are not simulated in a 1-D model, and the mean values for the two subreaches have an uncertainty of at least ±10%.

Figure 9 compares these mean values with model estimates for different TNS scenarios, with error bars corresponding to no correction and complete correction for change during the corresponding control runs. The near equilibrium of the subreach above Agassiz is reproduced fairly closely by the model with any plausible TNS. The model is also consistent with the survey-based estimate of aggradation below Agassiz if the natural sediment supply to middle Fraser River is around 0.4–0.5 Mt yr^{-1}. The interpretation of the control runs does not have a major influence on the agreement between model and data. Conversely, the comparison does not give a clear indication of the extent to which control run changes quantify model error.

The 47 year totals in Figure 9 can also be expressed as different estimates of the mean 1952–1999 gravel flux. The estimates from uncorrected mining runs are 0.11, 0.19, 0.29, and 0.39 Mt yr^{-1} for TNS 0.2, 0.3, 0.4, and 0.5 Mt yr^{-1} respectively; when corrected for changes during control runs, the estimates increase slightly to 0.14, 0.24, 0.35, and 0.46 Mt yr^{-1}. Either way, the two lowest TNS scenarios can again be rejected since, as noted earlier, the current fieldwork-based estimate of the gravel flux past Agassiz is 0.3–0.4 Mt yr^{-1}.

The scenarios with higher TNS are also more consistent with surface and subsurface GSDs measured in 1999–2000 at bar-head and midbar sites near Agassiz. The model active layer extends three grain diameters below the surface, i.e., to beneath any surface armor, so its cumulative GSD would be expected to plot between those for field pebble counts (coarser than model) and subsurface bulk samples (finer than model). The simulated 1999 GSDs with TNS 0.4 and 0.5 Mt yr^{-1} satisfy this test for all but the coarsest 10% or so of the distribution, but the 0.2 and 0.3 Mt yr^{-1} scenarios predict GSDs with higher D_{50} and D_{84} than the pebble counts. The predicted active layer D_{50} at Hope always falls between the measured surface and subsurface values of 100 mm and 30 mm [*McLean et al.*, 1999], and the predicted D_{50} at Lillooet is always appreciably coarser than the subsurface value quoted by *Ryder and Church* [1986].

6.2. Model Sensitivity to Tailings Supply

It might be expected that the simulated 1952–1999 behavior down river from the mining area would be sensitive to the assumed volume of tailings, but this is not the case. All results presented so far are for the central estimate of 58×10^6 m^3 (bulk volume, all sizes) in *Nelson and Church* [2012]. This estimate is based on the dimensions of mined hollows close to the river and has a 90% confidence interval of $55–62 \times 10^6$ m^3. *Nelson and Church* [2012] noted that the lower 90% bound would fall to 47×10^6 m^3 if locations mapped as "possibly mined" were excluded and that the upper bound might be higher if there are significant contributions from undetected mines or mines well up tributaries of Fraser River. We therefore tested the sensitivity of the 1858–1999 and 1952–1999 gravel budgets to a reduction of tailings supply by 22% to 45×10^6 m^3 (13 Mt less gravel than the central estimate) and an increase by 29% to 75×10^6 m^3 (16 Mt more gravel), in each case assuming a total natural supply of 0.4 Mt yr^{-1}. Simulated 1952–1999 gravel accumulation between Laidlaw and Agassiz changed by only ±0.1 Mt (±4%), and accumulation downstream from Agassiz by only −0.1/+0.2 Mt (±1%). These changes are not shown in Figure 9 because they would be invisibly small. The

main effect of a higher/lower tailings supply was instead within the mountains and within and soon after the mining period. The predicted impact of mining on lower Fraser River in the last half century is therefore robust to uncertainty about the precise volume of tailings.

6.3. River Response to Increased Sediment Supply

It is traditionally assumed that the initial response to an increase in sediment supply is aggradation, whether the increase is impulsive or sustained and is from point or dispersed sources. Much of the literature has focused on depths of aggradation and how they vary over time and space, with debate about the conditions which favor different combinations of translation or dispersion [*Lisle et al.*, 2001; *Cui et al.*, 2005; *Lisle*, 2008]. However, it is also possible to think about response in terms of grain size change. Flume experiments show that reduction in sediment supply narrows the bed load transport corridor [*Dietrich et al.*, 1989; *Nelson et al.*, 2009] and an increase in supply widens it [*Venditti et al.*, 2010a], until changes in surface character can no longer offset the change in supply and degradation or aggradation becomes inevitable. In the event of aggradation in such experiments, the topographic high translates only if the excess sediment is finer than the previous bed. The same is true of sediment pulses added without an upstream supply to simulate gravel augmentation below dams [*Sklar et al.*, 2009; *Venditti et al.*, 2010a; *Humphries et al.*, 2012]. *Gilbert* [1917], in his classic description of the effects of gold mining on rivers in California, talked of a sediment wave analogous to a flood wave, thus emphasizing translation, but he also found less aggradation farther downstream which indicates some dispersion, and *James* [1989] showed that the dispersion continued for more than a century. Initial translation followed by dispersion has also been documented experimentally, particularly for sediment pulses finer than the bed material [*Sklar et al.*, 2009; *Humphries et al.*, 2012].

Our simulations of the impact of gold mining on Fraser River suggest that the response was immediate and was characterized by strong sediment pulses rather than pronounced topographic waves. Two or more high-celerity pulses are apparent in the first few years but soon become smeared into a single wave of notably low amplitude: >2 m in a couple of topographically forced places but far below 1 m on average. This is much less aggradation than in other case studies of mining impact. *Gilbert* [1917] reported up to 5 m of channel aggradation as well as extensive deposition on floodplains, and *Knighton* [1989] estimated at least 6 m of aggradation in the Ringarooma River, Tasmania, in response to tin mining. The much lower amplitude of aggradation in our simulations is explained by three factors: (1) the total tailings supply to Fraser River was far less than in California and little more than in Tasmania; (2) while the tailings consisted mainly of gravel, they were finer grained than any part of the initial river bed; and, above all, (3) Fraser River is far bigger and more powerful than the rivers studied by Gilbert and Knighton. As noted earlier, gold mining along small tributaries of the Fraser upstream from Quesnel did lead to considerable aggradation.

We asserted at the start of this paper that any major increase in the supply of sediment to a river is offset by an increase in transport capacity, achieved by changes in one or more of channel slope, morphology, and bed characteristics. Previous studies of the effects of mining have identified all three responses: *Gilbert* [1917] saw an increase in slope through aggradation as the primary means to deal with an increase in sediment supply, but also reported channel widening, and *Knighton* [1989] found that aggradation was accompanied by transformation of a single-thread gravel bed river to a wider and braided sand bed river. Significant widening is impossible along most of the 370 km length of Fraser Canyon, so the only possible adjustments are aggradation and fining. A few meters of aggradation in a large river that drops 450 m over the relevant distance cannot alter slope and shear stress significantly, but fining of the bed surface gives an immediate reduction in threshold shear stress and thus an increase in transport rate. The non-wash load part of the tailings is 80% gravel, and simulated bed GSDs never contain more than 15% of sand, but the general fining of the bed is sufficient to increase bed load transport rates (as calculated using the equations of *Wilcock and Crowe* [2003]) by an order of magnitude at the peak of mining activity. This is consistent with the view that fine material accelerates sediment pulse and wave evolution by increasing transport rates [*Lisle et al.*, 2001; *Lisle*, 2008], and we note that mobilization of a coarse gravel bed by the addition of finer gravel has been demonstrated experimentally [*Venditti et al.*, 2010a, 2010b]. The documented field example that most nearly resembles our reconstruction is Elwha River in the northwest U.S., where dam removal added a large surcharge of sediment substantially finer than the coarse bed of a relatively steep (though much smaller) gravel bed river. The added sediment is being passed downstream to the river mouth with only limited aggradation (order 1 m) and bar building

[*East et al*., 2015]. The textural response (bed fining as fine-sediment supply increases, bed coarsening as it decreases) is also the same as observed by *Montgomery et al*. [1999] and *Gran et al*. [2006] following a volcanic eruption, though in that case there was also massive aggradation. These cases show that sediment caliber is a key factor determining river response to extraordinary sediment inputs and support the suggestion by *Ferguson* [2008, pp. 38–39] and *Buffington* [2012, p. 436] that GSD change is the fastest way in which alluvial rivers can adapt to changing conditions.

6.4. Morphodynamic Modeling With Sparse Information

A model that updates the longitudinal profile of a river and the bed GSD at all points along it has to start from some initial profile and GSDs. Information on these may be limited or nonexistent when, as in this paper, reconstructing river behavior more than a century ago; it may also be limited for modern rivers in remote regions or less developed countries. There may also be little or no information on one of the key boundary conditions: the supply of coarse sediment from inflows and side slopes.

Our novel approach to filling this information gap may be useful in other applications where the task is to simulate the effects of disturbances to a river that is initially in, or close to, equilibrium. The required longitudinal profile is that of the bed, not the water surface. We specified it as a smoothed version of the modern profile, but even in the absence of such ground data, it should be possible to estimate a water surface profile from detailed topographic maps, satellite imagery, or digital terrain models and then subtract water depths estimated by uniform flow calculations [*Magirl et al*., 2008; *Ronco et al*., 2009]. Specifying initial bed GSDs is more problematic, at least in gravel bed rivers where order-of-magnitude differences in mean diameter are possible and simulated transport rates are far more sensitive to grain size than is the case for sand bed rivers. Our procedure couples the specification of GSDs with that of sediment supply. The first stage is to identify a range of plausible scenarios of natural sediment supply (total quantity and spatial distribution). Next, for each supply scenario, bed GSDs at each node are optimized to give total bed load transport capacity equal to the cumulative supply from upstream of the node. Finally, for each scenario simulations are run with and without disturbance to the system. The effect of the disturbance is then expected to be somewhere within the range between the results of the disturbance run itself (if the model is assumed to be perfect) and the results of the disturbance run after subtracting changes in the control run (if the predisturbance river is assumed to have been in exact equilibrium).

This approach yields a range of predictions for the effect of the disturbance, because of uncertainty about the choice of supply scenario and how to interpret the control run, but it may be possible to narrow the range by using any available field evidence. In our case we were able to narrow the plausible range of total natural supply by using field evidence from the lower end of the model domain on aggradation rates, bed grain size, and gravel transport rates. In other historical reconstructions field or archival evidence of the vertical amplitude and/or timing of aggradation or degradation might help constrain a model.

7. Conclusions

We developed and ran a width-averaged morphodynamic model with multiple grain sizes to simulate changes in bed level, bed grain size distribution, and bed load transport rate along should be 522 km of Fraser River from 1858 to the present day in order to reconstruct the effects of gold mining which took place from 1858 to 1909 along all but the final 43 km of the model domain. The model necessarily involves several simplifications and speculative assumptions about processes and boundary conditions, because there is no information on the premining state of the river and little modern information about the first 500 km of the model domain. By comparing model predictions with the available modern data, and examining the simulated response to mining, we reach the following conclusions.

1. The model is able to match the empirical 1952–1999 sediment budgets for the subreaches from the mountain front at km 500 to km 522 and from km 522 to the gravel front ~35 km farther down river. It also matches the modern bed grain size distribution at km 522. This suggests that the model captures the effects of the main processes adequately.
2. To achieve this agreement with data, the total natural supply of sediment coarser than 0.5 mm must be of order 0.4–0.5 Mt yr^{-1}. Sediment finer than 0.5 mm travels almost continuously in suspension; that includes approximately half of the total mine tailings supply to the river.

3. The simulations suggest that around 90% of the gravel and coarse sand added as tailings left the mining area before the end of the mining period, and most of this was exported from the model domain. There was very little aggradation in and immediately beyond the mining region (mean elevation change far less than 1 m), in contrast to case studies of mining impact on rivers in California and Tasmania. The subdued topographic response and the rapidity of recovery from disturbance are consistent with the much greater size and power of Fraser River relative to the volume of added tailings.
4. The simulations show high-celerity sediment pulses (>10 km a^{-1}) in the first few years of mining, merging into a single large pulse or wave. Aggradation was modest because increases and decreases in sediment supply led immediately to increases and decreases in gravel transport rate, through fining and coarsening of the river bed. This was possible because, although most of the non-wash load part of the tailings sediment comprised gravel, not sand, it was finer than the premining river bed.
5. The simulations imply that there must have been a substantial advance of the gravel front, and aggradation in the last few tens of kilometers above it, during and soon after the mining period. They also suggest that gravel transport past Agassiz has been gradually increasing for several decades, as the postmining coarsening of the river bed is gradually reversed, and will continue to do so. This may have implications for the management of lower Fraser River.
6. Finally, our approach to setting up alternative initial states of the river may be useful in other attempts to model the effects of disturbances to rivers. We used it to create initial bed GSDs given some knowledge of the natural sediment supply rate, but it could also be used to estimate an unknown supply rate if observations of bed GSD are available. The approach has potential applications not just to human-induced disturbances but also to natural events such as sediment overload after earthquakes or eruptions.

Acknowledgments

Model details and results are freely available from Ferguson and information on the surveyed sediment budget data from Church (mchurch@geog.ubc.ca). We thank James Bomhof for the raft traverse GPS coordinates and smoothed water surface elevation series, Matt Chernos for the Google Earth measurements of river distances and widths, Nick Cox for advice on and help with LOWESS smoothing, Martin Lin for processing the canyon cross-section depths and velocities, and Eric Leinberger for constructing the diagrams. We thank Darwin Baerg and Fraser River Raft Expeditions for the raft traverse. The traverse was funded by a Natural Science and Engineering Research Council of Canada (NSERC) discovery grant to Church, and subsequent data processing was funded by NSERC discovery grants to Rennie and Venditti. Detailed comments from three anonymous reviewers, Associate Editor Amy East, and Editor John Buffington helped us refine the paper and set it into a wider context. Author contributions: R.I.F. constructed the model, devised the strategy, conducted all simulations and sensitivity tests, analyzed the results, and drafted most of the paper. M.C. suggested the modeling project, led the 2009 raft expedition, and helped draft the paper. C.R. and J.G.V. were in charge of data collection during the raft expedition, with additional help from Chris Adderly, and supervised subsequent extraction of GPS coordinates, water surface elevations, and canyon cross-section depths and velocities. All authors contributed to section 6 and helped edit the paper.

References

British Columbia Department of Mines (1946), *Notes on Placer Mining in British Columbia*, Bull., vol. 21, Charles F. Banyard (Government Printer), Victoria, B. C.

Buffington, J. M. (2012), Changes in channel morphology over human time scales, in *Gravel-Bed Rivers: Processes, Tools, Environments*, edited by M. Church, P. M. Biron, and A. G. Roy, pp. 435–463, Wiley, Chichester, U. K.

Church, M., D. G. Ham, and H. Weatherly (2001), Gravel management in lower Fraser River, Report for the City of Chilliwack, 40pp+36 figs. [Available at http://www.ibis.geog.ubc.ca/fraserriver/reports/.]

Cleveland, W. S. (1979), Robust locally weighted regression and smoothing scatterplots, *J. Am. Stat. Assoc.*, *74*, 829–836.

Cui, Y., and G. Parker (2005), Numerical model of sediment pulses and sediment-supply disturbances in mountain rivers, *J. Hydraul. Eng.*, *131*, 646–656.

Cui, Y., C. Paola, and G. Parker (1996), Numerical simulation of aggradation and downstream fining, *J. Hydraul. Res.*, *34*, 185–204.

Cui, Y., G. Parker, T. E. Lisle, J. Gott, M. E. Hansler-Ball, J. E. Pizzuto, M. E. Allmendinger, and J. M. Reed (2003), Sediment pulses in mountain rivers: 1. Experiments, *Water Resour. Res.*, *39*(9), 1239, doi:10.1029/2002WR001803.

Cui, Y., G. Parker, T. E. Lisle, J. E. Pizzuto, and A. M. Dodd (2005), More on the evolution of bed material waves in alluvial rivers, *Earth Surf. Processes Landforms*, *30*, 107–114.

Cui, Y., G. Parker, C. Braudrick, W. E. Dietrich, and B. Cluer (2006), Dam Removal Express Assessment Models (DREAM): Part 1. Model development and validation, *J. Hydraul. Res.*, *44*, 291–307.

Cui, Y., J. K. Wooster, J. G. Venditti, S. R. Dusterhoff, W. E. Dietrich, and L. S. Sklar (2008), Simulating sediment transport in a flume with forced pool-riffle topography: Examinations of two one-dimensional numerical models, *J. Hydraul. Eng.*, *134*, 892–904.

Dade, W. B., and P. F. Friend (1998), Grain size, sediment-transport regime, and channel slope in alluvial rivers, *J. Geol.*, *106*, 661–675.

Dietrich, W. E., J. W. Kirchner, H. Ikeda, and F. Iseya (1989), Sediment supply and the development of the coarse surface layer in gravel-bedded rivers, *Nature*, *340*(6230), 215–217.

East, A. E., et al. (2015), Large-scale dam removal on the Elwha River, Washington, USA: River channel and floodplain geomorphic change, *Geomorphology*, *228*, 765–786, doi:10.1016/j.geomorph.2014.08.028.

Ferguson, R. (2008), Gravel-bed rivers at the reach scale, in *Gravel-Bed Rivers VI*, edited by H. Habersack, H. Piégay, and M. Rinaldi, pp. 33–60, Elsevier, Amsterdam.

Ferguson, R. I., and M. Church (2004), A simple universal equation for grain settling velocity, *J. Sediment. Res.*, *74*, 933–937.

Ferguson, R. I., and M. Church (2009), A critical perspective on 1-D modeling of river processes: Gravel load and aggradation in lower Fraser River, *Water Resour. Res.*, *45*, W11424, doi:10.1029/2009WR007740.

Galois, R. M. (1970), Gold mining and its effects on landscapes of the Cariboo M.A. dissertation: 188pp.+10 foldout maps, The Univ. of Calgary, Calgary, Alberta, Canada.

Gilbert, G. K. (1917), Hydraulic mining debris in the Sierra Nevada, *U.S. Geol. Surv. Prof. Pap., 105*.

Gran, K. B., D. R. Montgomery, and D. G. Sutherland (2006), Channel bed evolution and sediment transport under declining sand inputs, *Water Resour. Res.*, *42*, W10407, doi:10.1029/2005WR004306.

Hickin, E. J. (1995), Hydraulic geometry and channel scour: Fraser River, B.C., Canada, in *River Geomorphology*, edited by E. J. Hickin, pp. 155–167, Wiley, Chichester.

Hoey, T. B., and R. Ferguson (1994), Numerical simulation of downstream fining by selective transport in gravel bed rivers: Model development and illustration, *Water Resour. Res.*, *30*, 2251–2260, doi:10.1029/94WR00556.

Humphries, R., J. G. Venditti, L. S. Sklar, and J. K. Wooster (2012), Experimental evidence for the effect of hydrographs on sediment pulse dynamics in gravel-bedded rivers, *Water Resour. Res.*, *48*, W01533, doi:10.1029/2011WR010419.

Ibbeken, H. (1983), Jointed source rocks and fluvial gravels controlled by Rosin's law: A grain size study in Calabra, South Italy, *J. Sediment. Petrol.*, *53*, 1213–1231.
James, L. A. (1989), Sustained storage and transport of hydraulic gold-mining sediment in the Bear River, California, *Assoc. Am. Geogr. Ann.*, *79*, 570–592.
Knighton, A. D. (1989), River adjustment to changes in sediment load: The effects of tin mining on the Ringarooma River, Tasmania, 1875–1984, *Earth Surf. Processes Landforms*, *14*, 333–359.
Kondolf, G. M., H. Piégay, and N. Landon (2002), Channel response to increased and decreased bedload supply from land use change: Contrasts between two catchments, *Geomorphology*, *45*, 35–51.
Lisle, T. E. (2008), The evolution of sediment waves influenced by varying transport capacity in hetereogeneous rivers, in *Gravel-Bed Rivers VI: From Process Understanding to River Restoration*, edited by H. Habersack, H. Piegay, and M. Rinaldi, pp. 443–472, Elsevier, Amsterdam.
Lisle, T. E., J. E. Pizzuto, H. Ikeda, F. Iseya, and Y. Kodama (1997), Evolution of a sediment wave in an experimental channel, *Water Resour. Res.*, *33*, 1971–1981, doi:10.1029/97WR01180.
Lisle, T. E., Y. Cui, G. Parker, J. E. Pizzuto, and A. M. Dodd (2001), The dominance of dispersion in the evolution of bed material waves in gravel-bed rivers, *Earth Surf. Processes Landforms*, *26*, 1409–1420.
Madej, M. A., and V. Ozaki (1996), Channel response to sediment wave propagation and movement, Redwood Creek, California, USA, *Earth Surf. Processes Landforms*, *21*, 911–927.
Madej, M. A., D. G. Sutherland, T. E. Lisle, and B. Pryor (2009), Channel responses to varying sediment input: A flume experiment modeled after Redwood Creek, California, *Geomorphology*, *103*, 507–519, doi:10.1016/j.geomorph.2008.07.017.
Magirl, C. S., M. J. Breedlove, R. H. Webb, and P. G. Griffiths (2008), Modeling water-surface elevations and virtual shorelines for the Colorado River in Grand Canyon, Arizona, *U.S. Geol. Surv. Sci. Invest. Rep., 2008–5075*, 32 pp.
McLean, D. G., and M. Church (1999), Sediment transport along lower Fraser River: II. Estimates based on the long-term sediment budget, *Water Resour. Res.*, *35*, 2549–2559, doi:10.1029/1999WR900102.
McLean, D. G., M. Church, and B. Tassone (1999), Sediment transport along lower Fraser River: I. Measurements and computations, *Water Resour. Res.*, *35*, 2533–2548, doi:10.1029/1999WR900101.
Montgomery, D. R., M. S. Panfil, and S. K. Hayes (1999), Channel-bed mobility response to extreme sediment loading at Mount Pinatubo, *Geology*, *27*, 271–274.
Nelson, A. D. (2011), The environmental history and geomorphic impact of 19th century placer mining along Fraser River, British Columbia MS dissertation, The Univ. of British Columbia: 141pp+2 foldout maps.
Nelson, A. D., and M. Church (2012), Placer mining along Fraser River, British Columbia: The geomorphic impact, *Geol. Soc. Am. Bull.*, *124*, 1212–1228, doi:10.1130/B30575.1.
Nelson, P. A., J. G. Venditti, W. E. Dietrich, J. W. Kirchner, H. Ikeda, F. Iseya, and L. S. Sklar (2009), Response of bed surface patchiness to reductions in sediment supply, *J. Geophys. Res.*, *114*, F02005, doi:10.1029/2008JF001144.
Nicholas, A. P., P. J. Ashworth, M. J. Kirkby, M. G. Macklin, and T. Murray (1995), Sediment slugs: Large-scale fluctuations in fluvial transport rates and storage volumes, *Prog. Phys. Geogr.*, *19*, 500–519.
Parker, G. (1990), Surface-based bedload transport relation for gravel rivers, *J. Hydraul. Res.*, *28*, 417–436.
Parker, G. (2004), 1D sediment transport morphodynamics with applications to rivers and turbidity currents e-book, chapter 14. [Available at http://hydrolab.illinois.edu/people/parkerg//morphodynamics_e-book.htm.]
Rice, S. P., and M. Church (2010), Grain-size sorting within bars in relation to downstream fining along a wandering channel, *Sedimentology*, *57*, 232–251, doi:10.1111/j.1365-3091.2009.01108.x.
Ronco, P., G. Fasolato, and G. Di Silvio (2009), Modelling evolution of bed profile and grain size distribution in unsurveyed rivers, *Int. J. Sediment. Res.*, *24*, 127–144.
Rosin, P., and E. Rammler (1933), Laws governing the fineness of powdered coal, *J. Inst. Fuel*, *7*, 29–36.
Ryder, J. M., and M. Church (1986), The Lillooet terraces of Fraser River: A palaeoenvironmental enquiry, *Can. J. Earth Sci.*, *23*, 869–884.
Shih, S.-M., and P. D. Komar (1990), Differential bedload transport rates in a gravel-bed stream: A grain-size distribution approach, *Earth Surf. Processes Landforms*, *15*, 539–552.
Simon, A., and C. R. Thorne (1996), Channel adjustment of an unstable coarse-grained stream: Opposing trends of boundary and critical shear stress, and the applicability of extremal hypotheses, *Earth Surf. Processes Landforms*, *21*, 155–180.
Sklar, L. S., J. Fadde, J. G. Venditti, P. Nelson, M. A. Wydzga, Y. Cui, and W. E. Dietrich (2009), Translation and dispersion of sediment pulses in flume experiments simulating gravel augmentation below dams, *Water Resour. Res.*, *45*, W08439, doi:10.1029/2008WR007346.
Stecca, G., A. Siviglia, and A. Blom (2014), Mathematical analysis of the Saint-Venant-Hirano model for mixed-sediment morphodynamics, *Water Resour. Res.*, *50*, 7563–7589, doi:10.1002/2014WR015251.
Sutherland, D. G., M. H. Ball, S. J. Hilton, and T. E. Lisle (2002), Evolution of a landslide-induced sediment wave in the Navarro River, California, *Geol. Soc. Am. Bull.*, *114*, 1036–1048.
Venditti, J. G., and M. Church (2014), Morphology and controls on the position of a gravel-sand transition: Fraser River, British Columbia, *J. Geophys. Res. Earth Surf.*, *119*, 1959–1976, doi:10.1002/2014JF003147.
Venditti, J. G., W. E. Dietrich, P. A. Nelson, M. A. Wydzga, J. Fadde, and L. Sklar (2010a), Effect of sediment pulse grain size on sediment transport rates and bed mobility in gravel bed rivers, *J. Geophys. Res.*, *115*, F03039, doi:10.1029/2009JF001418.
Venditti, J. G., W. E. Dietrich, P. A. Nelson, M. A. Wydzga, J. Fadde, and L. Sklar (2010b), Mobilization of coarse surface layers in gravel-bedded rivers by finer gravel bed load, *Water Resour. Res.*, *46*, W07506, doi:10.1029/2009WR008329.
Venditti, J. G., C. D. Rennie, J. Bomhof, R. W. Bradley, M. Little, and M. Church (2014), Flow in a bedrock canyon, *Nature*, *513*, 534–537, doi:10.1038/nature13779.
Viparelli, E., D. Gaeuman, P. Wilcock, and G. Parker (2011), A model to predict the evolution of a gravel bed river under an imposed cyclic hydrograph and its application to the Trinity River, *Water Resour. Res.*, *47*, W02533, doi:10.1029/2010WR009164.
Wilcock, P. R., and J. C. Crowe (2003), Surface-based transport model for mixed-size sediment, *J. Hydraul. Eng.*, *129*, 120–128.